Eur. Phys. J. B **12**, 115–118 (1999)

THE EUROPEAN PHYSICAL JOURNAL B

EDP Sciences

Effective scaling behavior of magnetization and Hamming distance in Ising thin films under a surface field

E.M. de Sousa Luz[1,a], A.F. Siqueira[1], U.M.S. Costa[1], and M.L. Lyra[2,b]

[1] Departamento de Física, Universidade Federal do Ceará, 60470-455 Fortaleza CE, Brazil
[2] Departamento de Física, Universidade Federal de Alagoas, 57072-970 Maceió AL, Brazil

Received 29 March 1999 and Received in final form 21 April 1999

Abstract. The recent improvements on the technology for developing high-quality thin magnetic films has renewed the interest in the study of surface effects in both static and dynamic magnetic responses. In this work, we use a Monte-Carlo algorithm with Metropolis dynamics together with a spreading of damage technique to study the interplay between the effects of finite thickness and surface ordering field in thin ferromagnetic Ising ($S = 1/2$) films. We calculate, near the bulk critical temperature and several values of the surface field, the dependence on the film thickness of the average magnetization M and Hamming distance D. We employ a finite size scaling analysis to show that both obey an effective one-parameter scaling but exhibit distinct characteristic surface fields. At their corresponding characteristic surface fields both M and D become roughly thickness independent and we estimate the critical exponent characterizing the behavior of the typical scaling lengths.

PACS. 75.70.Ak Magnetic properties of monolayers and thin films – 75.40.Mg Numerical simulation studies – 75.40.Cx Static properties (order parameter, static susceptibility, heat capacities, critical exponents, etc.)

1 Introduction

The effects of surfaces on the critical behavior of layered magnetic structures have been studied intensively in the past years [1]. The increasing interest in the understanding of finite-size and surface effects on films is mainly due the recent improvements in the experimental techniques for preparing high quality thin films. Such systems include magnetic overlayers, sandwiches and superlattices, displaying a great variety of unusual properties [2]. The presence of free surfaces, which may be subject to surface fields due to substrates or adjacent magnetic layers, leads to non-homogeneous behavior in the film which makes the determination of the bulk properties particularly difficult [3].

In the theory of phase transitions on Ising films with free surfaces, the spins on the surface layers are generally supposed to interact with each other with an exchange integral J_s different from the bulk exchange integral J_b and/or to be under the action of surface ordering fields [4]. Therefore, there is a competition between the finite thickness effect which favors the disordered phase and the ordering effects due to these surface enhancing operators. For example, for J_s above a critical value $J_{sc} > J_b$, the system orders on the surface before it becomes ordered in the bulk [5]. Also, the unusual behavior of the specific heat of free-standing liquid crystal films [6] has been related to the interplay between surface ordering and finite size effects [7,8]. So far, attention has been focused mainly on static properties. However, near a critical point a variety of dynamic critical phenomena, such as the critical slowing down, also occur [9]. Since surface effects modify the critical behavior of local static quantities as the order parameter density near the surface, a natural question that arises is about its possible effects on local *dynamic* properties [10].

On the other hand, the spreading of damage technique has been widely used to study the critical properties of Ising-like systems [11–13]. This technique is based on the synchronous Monte-Carlo update of two distinct spin configurations which initially differ on a given set of lattice sites. The Monte-Carlo updates are identical in the sense that the same set of random numbers is used to update each spin configuration. As the Ising model does not have an intrinsic dynamics, it is chosen as a particular one, commonly among the Metropolis, Glauber and heat-bath dynamics. The results depend to a great extent on the dynamics chosen as opposed to what occurs in the usual statistical Monte-Carlo modeling [14]. The Hamming distance D is defined as the fraction of spins that are different in the two configurations averaged along the Markov

[a] *Permanent address*: Universidade Estadual do Piauí, 64002-150 Teresina PI, Brazil.
[b] e-mail: marcelo@ising.fis.ufal.br

chain. It displays a critical behavior at the so called critical spreading temperature $T_{\rm s}$. Recently, the spreading of damage technique with the Metropolis dynamics was used to study a layered $S = 1/2$ Ising ferromagnetic thin film with an enhanced surface coupling constant [15]. The temporal evolution of the damage front was followed and two distinct spreading regimes were found near and above the bulk critical spreading temperature.

Throughout this paper, we investigate the behavior of layered $S = 1/2$ Ising ferromagnetic thin film subject to a magnetic field in both free surfaces. We will study as the magnetization changes with the film thickness and the applied surface field. We will use the Monte-Carlo simulation with Metropolis dynamics. Besides this, we will apply the spreading of damage technique based also on the Metropolis algorithm in order to compare the Hamming distance behavior with the magnetization at the bulk critical temperature. The outline of the paper is as follows: In Section 2 we will define the model and the Metropolis dynamics in the context of the spreading of damage technique. Section 3 deals with the evolution of the magnetization and the Hamming distance in function of the magnetic field and the film thickness, for a lattice with $L \times L \times N$ sites near criticality. Finally, in Section 4, we will summarize our conclusions.

2 The model and the Metropolis algorithm

Let us consider the nearest-neighbor interaction Ising ferromagnet ($S = 1/2$) on a layered geometry with a magnetic field $H_{\rm s}$ applied in both free surfaces. The Hamiltonian can be written in the following general form:

$$\mathcal{H} = -\sum_{\lambda=1}^{N-2}\sum_{\langle i,j\rangle} J_{\rm b}\, S^z_{i,\lambda}S^z_{j,\lambda} - \sum_{\alpha=1}^{2}\sum_{\langle l,m\rangle} J_{\rm s}\, S^z_{l,\alpha}S_{m,\alpha} - H_{\rm s}\sum_{\alpha=1}^{2}\sum_{l} S_{l\cdot\alpha} - \sum_{\nu=1}^{N-1}\sum_{p} J_t\, S^z_{p\nu}S^z_{p\nu+1}, \qquad (1)$$

where N is the total number of the layers. The first sum corresponds to the spin interactions within the inner layers, the second sum is the contribution of the surface spin interactions, the third one corresponds to the interaction between the external field and all the spins in both the top and bottom surfaces. Finally the fourth one is the interaction energy between adjacent layers. In what follows, we will consider only physical situations where $J_{\rm b} = J_{\rm s} = J_t = J$ but keep a positive surface field $H_{\rm s}$. To approximate the infinite system by the finite lattice we use periodic boundary conditions for those directions in which the crystal is infinite, keeping free boundary conditions for both surfaces of the film. The linear size of the system considered in our simulation was $20 \times 20 \times N$ and $40 \times 40 \times N$, with N ranging from 3 up to 12 layers. We performed $L \times L \times N$ ($L = 20, 40$) Monte-Carlo steps per spin (MCS/spin) in order to achieve thermal equilibrium of an initial random spin configuration. We use Metropolis dynamics in the sense that each spin is flipped with probability:

$$p_i(t) = \min(1, {\rm e}^{-2\beta S_i h_i(t)}), \qquad (2)$$

where $\beta = 1/k_{\rm B}T$ and $h_i(t) = (J+H')\sum_j S_j(t)$. $H' = H_{\rm s}$ if the spin belongs to a surface layer and is equal to zero otherwise. Once thermal equilibrium is reached we calculate the magnetization and average over $L \times L \times N/3$ different initial configurations for the same value of temperature. At the same time, *i.e.* in thermal equilibrium , a copy of the spin configuration is made and one flips one of its spins belonging to a randomly chosen layer. Both copies are let to evolve along the Markov chain governed by the same random numbers. In order to investigate the equilibrium properties of the Hamming distance, we let both copies to evolve under the above dynamical rules for an additional $L \times L \times N$ MCS/spin. After that, we compare the two configurations A and B and evaluate the microscopic Hamming distance given by:

$$\langle D(t)\rangle \;=\; \frac{1}{4N'}\sum_i \langle (S_i^A(t) - S_i^B(t))^2\rangle, \qquad (3)$$

where A and B indicate, respectively, the thermalized lattice and its image, N' is the number of sites and the brackets represent the configurational average over a large number of subsequent spin configurations. We usually took $L\times L\times N/3$ additional configurations. The damage is reintroduced whenever the two configurations become identical or symmetrical [15].

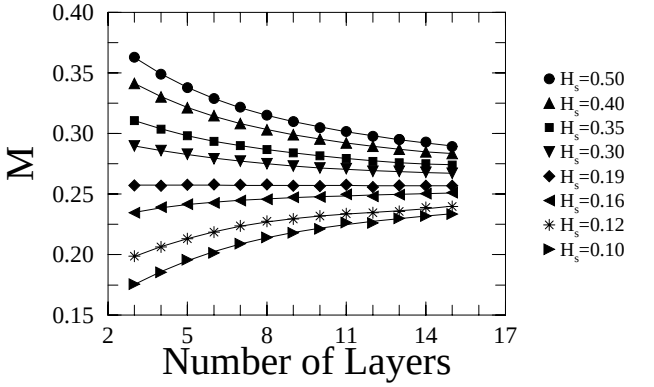

Fig. 1. The average magnetization M *versus* the number of layers (N) for several surface magnetic fields at the bulk critical temperature.

3 The magnetization and Hamming distance thickness dependence

At first, we study the thickness dependence of the magnetization near the critical temperature of the bulk Ising model ($k_{\rm B}T/J = 1.095$) for several values of the surface magnetic field ($H_{\rm s}$ ranging from 0.10 to 0.50). Our results are shown in Figure 1. Data are from Monte-Carlo runs on lattices with $20 \times 20 \times N$ sites. We also

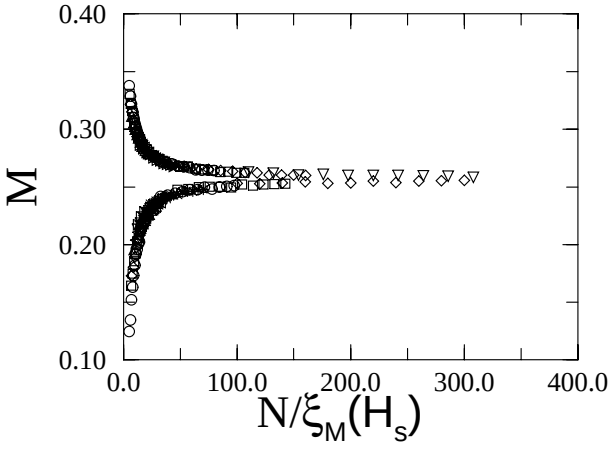

Fig. 2. Data collapse of the magnetization *versus* N curves. Data from $H_{\rm s} = 0.05$ and $H_{\rm s} = 0.50$ were used as reference. The scaling lengths ξ_M were estimated in order to obtain the best data collapse. Different symbols stand for different N.

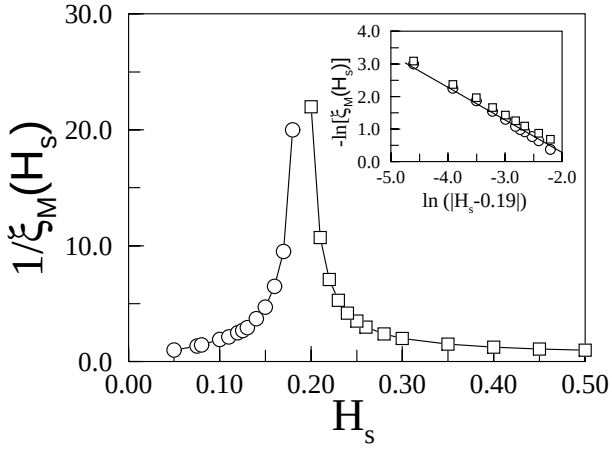

Fig. 3. $1/\xi_M$ *versus* $H_{\rm s}$ for the average magnetization. In the inset we show the power-law behavior near $H_{\rm s}^* = 0.19$. The straight line has slope 1.

performed a few runs on lattices with $40 \times 40 \times N$ which presented similar results. We observe that for $H_{\rm s}$ lower than a characteristic value $H_{\rm s}^* = 0.19$ the average total magnetization (M) increases when the number of layers is increased showing the predominant role played by the finite thickness which favors large spin fluctuations. For $H_{\rm s} > H_{\rm s}^*$ the surface ordering becomes predominant and M decreases with the layers number changing its concavity. At $H_{\rm s} = H_{\rm s}^*$ finite size and surface ordering effects are balanced and M becomes roughly independent of the number of layers. The above behavior can be described as an underlying correction to scaling due to a change in sign of a L-dependent term as the surface field is increased. However, if we concentrate our attention on the range of surface fields around $H_{\rm s}^*$, the above picture can effectively be considered as the typical finite-size scaling behavior of a zero-exponent quantity. Following standard finite size scaling arguments, the average magnetization is considered to obey a one-parameter scaling on the form

$$M = f_{\pm}[N/\xi_M(H_{\rm s})], \tag{4}$$

with $\xi_M(H_{\rm s}) \sim |H_{\rm s} - H_{\rm s}^*|^{\Phi}$ representing the characteristic thickness governing the approach of the magnetization to its thermodynamic limit. For $N \ll \xi_M$ the average magnetization is strongly sensitive to the presence of the surfaces while for $N \gg \xi_M$ the magnetization becomes thickness independent. $f_{\pm}$ are distinct scaling functions for surface fields higher (+) and lower (−) than the characteristic field $H_{\rm s}^*$. $M(H_{\rm s} = H_{\rm s}^*) = f_{\pm}(\infty)$ independent of the film thickness. In Figure 2, we employ a data collapse of the $M \times N$ curves choosing the data from $H_{\rm s} = 0.05$ and $H_{\rm s} = 0.50$ as reference curves below and above $H_{\rm s}^*$ respectively. The $\xi_M(H_{\rm s})$ values are estimated in order to obtain the best data collapse. In Figure 3, we plot the so obtained dependence of ξ_M on $H_{\rm s}$ which shows a power-law behavior near $H_{\rm s} = H_{\rm s}^* = 0.19$ with $\Phi = 1.0 \pm 0.1$.

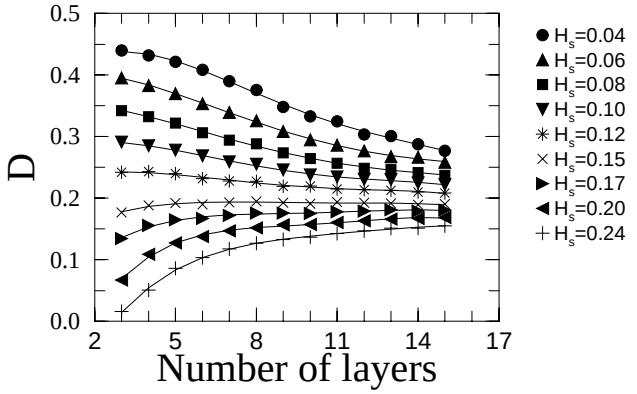

Fig. 4. The Hamming distance (D) *versus* the number of layers (N) for several surface magnetic fields at the bulk critical temperature.

We applied the above analysis about the interplay between thickness and surface field on the average Hamming distance in the stationary regime. We observe a very similar behavior with D displaying a roughly thickness independent behavior at a characteristic surface field and distinct trends for lower and higher fields (see Fig. 4). However the trends are reversed as compared to the magnetization behavior. This is related to the fact that, within the Metropolis dynamics, the damage is more likely to spread in the absence of long-range order and therefore a strong surface ordering field suppress the Hamming distance. A second relevant point is that the characteristic surface field is $H_{\rm s}^* = 0.15$, about 20% lower than the one obtained for the magnetization. Following the same procedure used to obtain the effective surface scaling behavior of M, we collapse the Hamming distance data onto a scaling form (see Fig. 5)

$$D = g_{\pm}[N/\xi_D(H_{\rm s})] \quad , \tag{5}$$

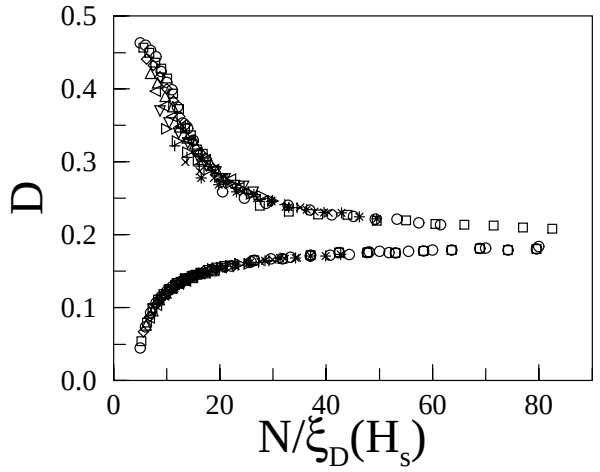

Fig. 5. Data collapse of the Hamming distance *versus* N curves. Data from $H_s = 0.01$ and $H_s = 0.28$ were used as reference. The scaling lengths ξ_M were estimated in order to obtain the best data collapse. Different symbols stand for different N.

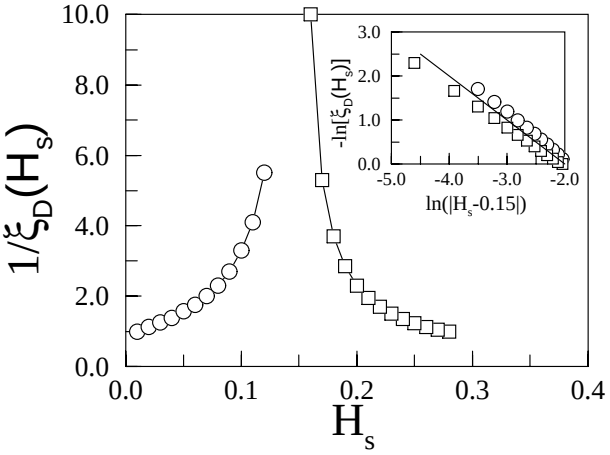

Fig. 6. $1/\xi_D$ *versus* H_s for the Hamming distance. In the inset we show the power-law behavior near $H_s^* = 0.15$. The straight line has slope 1.

with the estimated field dependence of ξ_D shown in Figure 6. It also shows a power-law behavior near $H_s^* = 0.15$ with $\Phi = 1.0 \pm 0.1$.

4 Conclusions

In this work we have investigated the critical behavior of the magnetization and Hamming distance in $S = 1/2$ Ising layered films under the presence of a magnetic field applied to both free surfaces. We showed that these quantities exhibit an effective scaling behavior as a function of the film thickness. The scaling behavior is characterized by the existence of a typical length scale that governs the interplay between finite thickness and surface ordering field effects. At a characteristic surface field this typical length scale vanishes reflecting the fact that, at this point, finite thickness and surface ordering effects are balanced in such a way that the order parameter becomes thickness independent. We obtained that the characteristic surface field for the Hamming distance is somewhat lower than the one for the magnetization. We should point out here that it has been well established in the literature that static and dynamic phase transitions may present distinct critical parameters [16–18] as is the case reported in the present work. However, we obtained that the vanishing of the typical length scales are characterized by the same critical exponent for both static and dynamic responses. A very natural extension of the present work is to investigate the possible existence of a dynamical counterpart to the wetting-like transition in Ising films which appears when competing surface and bulk ordering fields are present [19–21]. We are currently working along this direction.

This work was partially supported by CNPq, CAPES and FINEP (Brazilian agencies). The research work of E.M.S.L. is supported by a studentship from CNPq.

References

1. For background information and an extensive list of references see: K. Binder, Critical behavior at surfaces in *Phase Transition and Critical Phenomena*, edited by C. Domb, J.L. Lebowitz (New York, Academic Press, 1983), Vol. 8.
2. See, *e.g.*, S.D. Bader, Proc. of IEEE **78**, 909 (1990), and references therein.
3. H. Naganishi, M.E. Fisher, J. Chem. Phys. **78**, 3279 (1983).
4. H.W. Diehl, Int. J. Mod. Phys. B **11**, 3503 (1997).
5. K. Binder, P.C. Hohenberg, Phys. Rev. B **6**, 3461 (1972).
6. R. Geer, T. Stoebe, C.C. Huang, Phys. Rev. B **45**, 13055 (1992).
7. H. Li, M. Paczuski, M. Kardar, K. Huang, Phys. Rev. B **44**, 8274 (1991).
8. M.L. Lyra, Phys. Rev. B **47**, 2501 (1993).
9. H.W. Diehl, J. Appl. Phys. **53**, 435 (1982).
10. S. Dietrich, H.W. Diehl, Z. Phys. B **51**, 343 (1983).
11. M. Creutz, Ann. Phys. **167**, 62 (1986).
12. H.E. Stanley, D. Stauffer, J. Kertész, H.J. Herrmann, Phys. Rev. Lett. **59**, 2326 (1987).
13. For a review see, *e.g.*, N. Jan, L. de Arcangelis, Ann. Rev. Comput. Phys. **1**, 1 (1994).
14. R.M.C. de Almeida, J. Phys. I France **3**, 951 (1993).
15. A.V. Lima, M.L. Lyra, U.M.S Costa, J. Magn. and Magn. Mater. **171**, 329 (1997).
16. U.M.S. Costa, J. Phys. A **20**, L583 (1987).
17. G. le Caër, Physica A **159**, 329 (1989).
18. P. Grassberger, J. Phys. A: Math. Gen. **28**, L67 (1995).
19. H. Nakanishi, M.E. Fisher, Phys. Rev. Lett. **49**, 1565 (1982).
20. K. Binder, D.P. Landau, Phys. Rev. B **46**, 4844 (1992)
21. D.P. Landau, K. Binder, J. Magn. and Magn. Mater. **104-107**, 841 (1992).